

## Conference Paper

# Behaviour of Ion-modified Cladding Tubes from E110 Alloy in High-temperature Water Steam

**Alexander Yashin, Denis Safonov, Boris Kalin, Nikolay Volkov, Dmitriy Alexandrov, and Egor Korenevskiy**

National Research Nuclear University MEPhI (Moscow Engineering Physics Institute), Department of Physical problems of materials science, Kashirskoe shosse 31, Moscow, 115409, Russia

## Abstract

A series corrosion tests was carried out on 10 mm long samples of fuel tubes made of the E110opt alloy in a steam at the temperature of 800 °C for 5000 s. The samples were studied in the initial state, after ion polishing, alloying of the surface layer with Fe, Fe+Mo, Fe+Y, Cr, Mg and Al atoms by ion mixing. It is shown that the ion polishing of samples by argon ions, using the chosen regime, reduces the overweight in the high-temperature oxidation (HTO) under the 800/5000 regime from 2.090 to 1.730 mg/cm<sup>2</sup>, respectively. A series of works on modifying the surface by ion polishing and subsequent alloying with Fe, Fe+Mo, Fe+Y, Cr, Mg and Al atoms by ion mixing was carried out on the installation ILUR-03. It is shown that under the HTO conditions, the best results were obtained in case of alloying with Fe atoms as applied to the 800/5000 oxidation regime. At that, the overweight decreased from 2.090 to 1.900 mg/cm<sup>2</sup>. It is shown that the highest resistance under the HTO conditions was obtained for the FeCrNi coating: under the 800/5000 regime, the overweight decreased from 2.090 to 1.720 mg/cm<sup>2</sup>; under the 800/7500 regime - from 3.250 to 2.450 mg/cm<sup>2</sup>; and under the 1000/5000 regime - from 5.340 to 5.140 mg/cm<sup>2</sup>.

Corresponding Author:

Alexander Yashin  
 yashin\_itf@mail.ru

Received: 21 December 2017

Accepted: 15 April 2018

Published: 6 May 2018

Publishing services provided by  
**Knowledge E**

© Alexander Yashin et al. This article is distributed under the terms of the [Creative Commons Attribution License](#), which permits unrestricted use and redistribution provided that the original author and source are credited.

Selection and Peer-review under the responsibility of the MIE-2017 Conference Committee.

## 1. INTRODUCTION

Investigation of WWER fuel behavior in loss of coolant accident (LOCA) conditions is actual goal. One of the most destructive factors, affecting on fuel rods in LOCA conditions, is active oxygen penetration into the zirconium claddings from water steam environment, catastrophically fast oxide growth. Oxide layer often has a loose structure and has no protective properties, does not inhibit oxygen and hydrogen penetration into the metal. Oxygen and hydrogen penetrated contribute to alloy embrittlement. That is why research of ways to increase of fuel rods lifetime is going on actively.

 **OPEN ACCESS**

For example, one of concepts is accident tolerant fuel (ATF) development in following areas: modification of zirconium fuel claddings near-surface layers; protection of material by means of various coatings (for example, Cr); replacement of zirconium alloys for corrosion-resistant steels or composite SiC || SiC.

As one of possible ways to improve resistance of zirconium alloys used against high-temperature oxidation (HTO) ion-beam modification of fuel cladding surface is considered in this paper. First, it changing of phase and structure state of near surface layers by alloying in mode of ion mixing of atoms from substrate and film deposited, second – deposition of protective ion-assisted coatings in complex mode of deposition and ion irradiation.

## 2. MATERIALS AND TOOLS

Ion-beam modification was performed on fuel claddings parts 9.15 mm outer diameter 200...500 mm length made from E110opt alloy (Zr-1%Nb) based on sponge Zr (Figure 1). Initial and modified specimens cut into the 10 mm length rings before further corrosion tests and diagnostic.



**Figure 1:** Specimens from E110opt alloy for investigations.

Specimens' outer surface was modified on installation for complex ion-beam treatment of long-range products ILUR-03 (Figure 2). On first stage, surface cleaning and polishing (up to  $Ra < 0.3 \mu\text{m}$ ) was performed by radial polyenergetic  $\text{Ar}^+$  ions beam 3-4 keV average energy, that forms by sectioned cylindrical anode with 100 mm length active area.

Modification of structural phase state was carried out as follows. Films of alloying elements in combinations Fe, Fe+Mo, Fe+Y 10-100 nm total thickness were deposited on ion polished surface by three magnetron sputtering systems. Than composition "film-substrate" was irradiated by  $\text{Ar}^+$  ions (in ion mixing mode) to implant ("drive in") atoms from film in substrate lattice. Ion current was varied within 5-10 mA, total irradiation dose -  $(1-10) \times 10^{18}$  ion/cm<sup>2</sup>, surface temperature does not exceed 150 °C.

Modification by deposition of coatings 2...8  $\mu\text{m}$  thickness from Cr and FeCrNi atoms was carried out by magnetrons on installations KVK-10 and ILUR-03 respectively [1, 2]. As can be seen from Figure 3, there are cassette unit with vertical specimens position inside KVK-10 vacuum chamber. The coating is deposited over the entire length of the

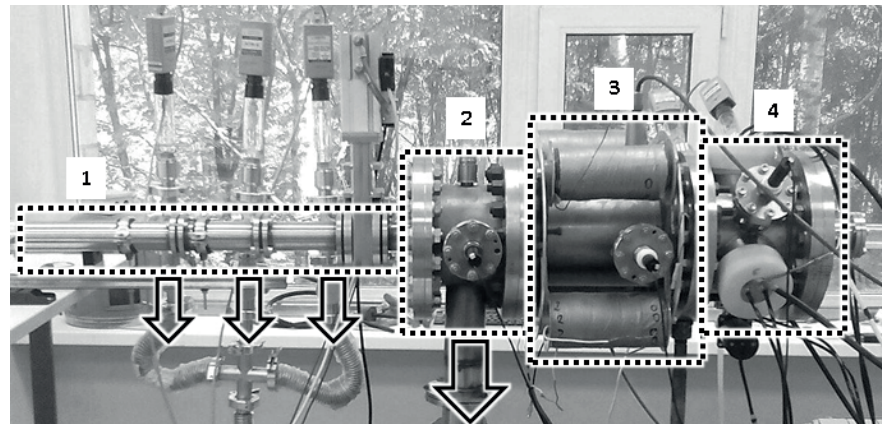


**Figure 2:** Installation ILUR-03: 1 - gateway vacuum chamber; 2 - preliminary evacuation chamber; 3 - zone radial ion beam action; 4 - zone of films deposition; the arrows show the pipelines of the vacuum system.

claddings fragments by means of wide-aperture magnetrons. Substrates surface was preliminary treated by Ar<sup>+</sup> ions from built-in ion source.



**Figure 3:** Installation KVK-10 (a) and its main chamber with cassette unit for 6 specimens (b).

Initial and modified specimens were oxidized on installation "GASPAR" [3] in mixture argon-water steam at temperature 800 °C up to 5000 s (800/5000 mode), up to 7500 s (800/7500), at temperature 1000 °C up to 5000 s (1000/5000s). Some specimens were preliminary autoclaved in standard conditions – water temperature 350 °C, pressure 16.5 MPa up to 400 h. The degree of claddings oxidation was estimated from the specific weight gain and ECR parameter (equivalent cladding reacted). The last one was determined by calculation as ratio of the total thickness of an equivalent layer of zirconium (which would react with steam) to the initial thickness of the shell [3]:

$$ECR = N \times \delta e \times \delta_0^{-1} \times 100\%, \quad (1)$$

where ECR – equivalent cladding reacted, %;  $N$  – coefficient concerns with double-sided cladding oxidation,  $N = 2$ ;  $\delta e$  – equivalent layer thickness (calculated thickness of zirconium, which would go to ZrO<sub>2</sub> formation);  $\delta_0$  – initial specimen thickness. Gravimetric data obtain on analytical scale A&D GH-252 0.01 mg sensitivity.

The relief of initial and modified surfaces was studied using a contact profilometer TR-200 on base length 1.0 mm with 0.5  $\mu\text{m}$  step. Surface state and oxide layer transverse structure was studied by scanning electron microscope Carl Zeiss EVO 50 with a guaranteed resolution up to 3 nm after the metallographic sections preparation. The device is equipped with prefixes for X-ray spectral analysis of the samples surface elemental composition using energy dispersive and wave dispersion spectrometers (EDS, WDS). The depth of the characteristic radiation output did not exceed 2  $\mu\text{m}$ .

### 3. RESULTS

As preliminary steam corrosion tests results show, there are a lot of large cracks in oxide film on samples from E110opt alloy grown up at 800  $^{\circ}\text{C}$ , which can be seen on Figure 4. They strongly increase diffusion rate of oxygen into the metal. Cracks formation is possibly concern with changes of samples changes, taking place during phase transition in zirconium. As can be seen from diagram Zr-Fe, shown on Figure 5, even with an insignificantly low iron content as an additive, the temperature of polymorphic  $\alpha \leftrightarrow \beta$  conversion in doped zirconium decreases from 862 to 795  $^{\circ}\text{C}$  [4].

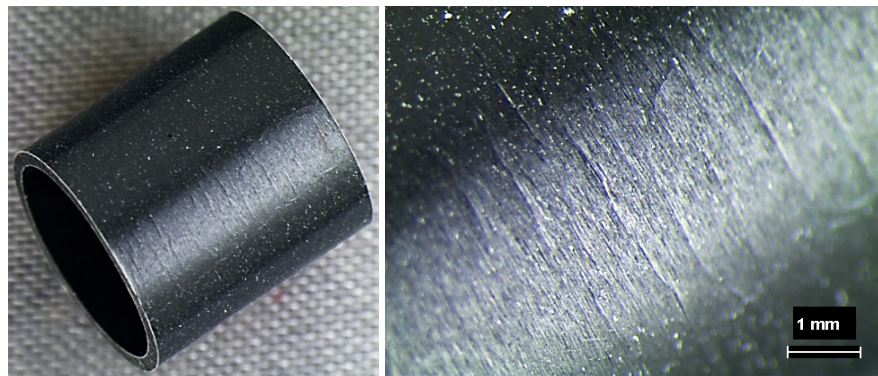


**Figure 4:** Typical photos of sample from E110opt alloy in initial state after steam oxidation at 800  $^{\circ}\text{C}$  during 5000 s.

#### Ion polished samples

As a result atoms of ion sputtering, definite relief is formed on the alloy surface. As can be seen from the profilograms shown on Figure 6, the ion-polished surface has a smoother relief compared to the initial state, the average value of the roughness parameter is  $R_a = 0.2 \pm 0.1 \mu\text{m}$ .

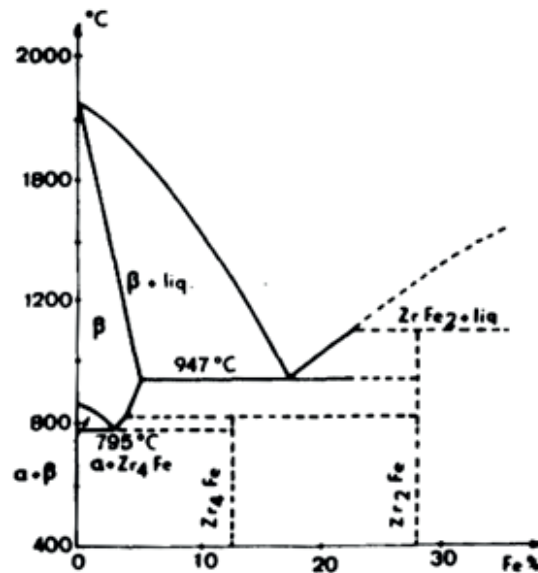


Figure 5: Part of the system Zr-Fe phase diagram.

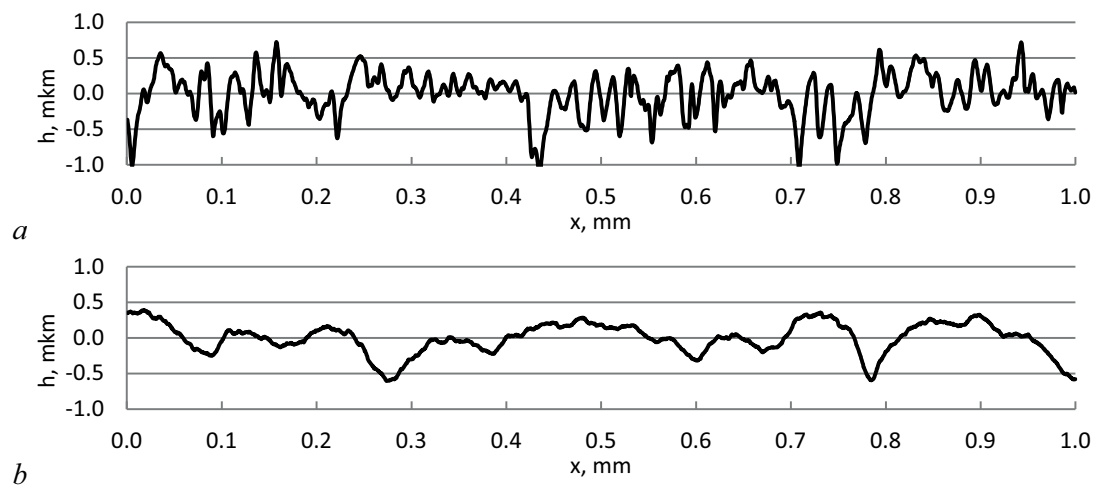
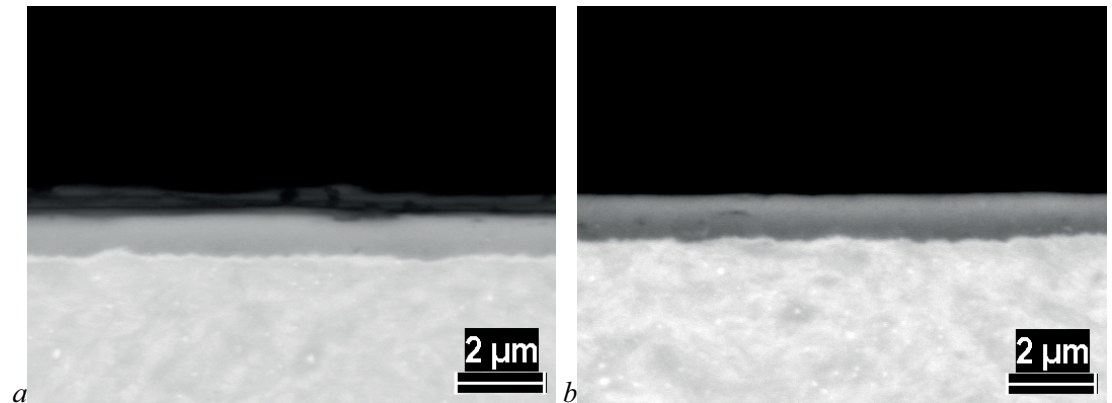


Figure 6: Typical profilograms of the outer surface of the samples in initial state (a) and after ion polishing (b).

## Autoclaving

As a result of autoclaving, an oxide film of uniform dark color is formed on the initial and ion-polished samples without visible traces of destruction. In this case, the average value of the total specific weight gain is  $0.14 \pm 0.02 \text{ mg/cm}^2$  for the samples in the initial state, and for the ion-polished samples, on the average, twice less -  $0.07 \pm 0.02 \text{ mg/cm}^2$ . Analysis of the transverse structure of oxides by metallography and scanning electron microscopy showed that the average value of the oxide film on the surface of the initial samples is  $1.5 \pm 0.1 \mu\text{m}$  and, as can be seen at Figure 7a, has a definite two-layer structure with an outer loose oxide layer of thickness  $0.4 \pm 0.1 \mu\text{m}$ . The oxide on the

surface of ion-polished samples, as seen on Figure 8b, has a thickness of  $1.0 \pm 0.1 \mu\text{m}$  and shows a dense structure with an insignificant number of discontinuities.



**Figure 7:** Typical SEM-images of transverse sections prepared on samples in the initial state (*a*) and after ion polishing (*b*) after autoclave testing.

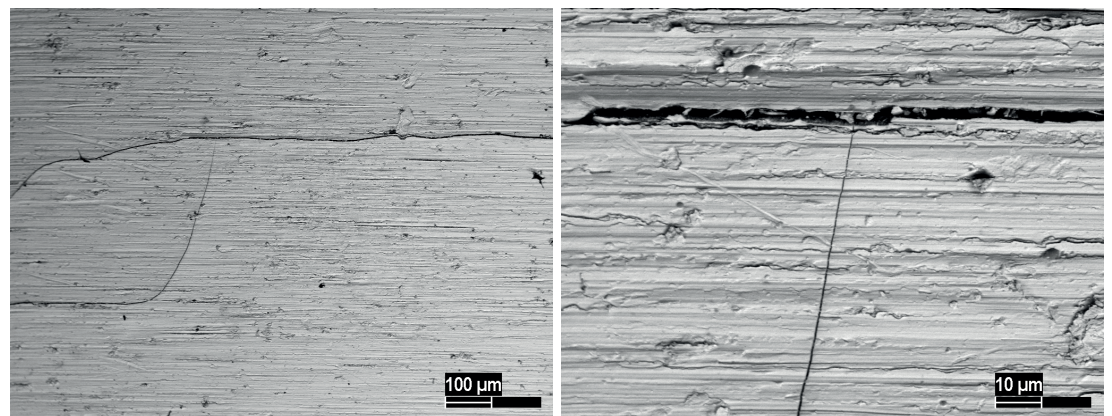


**Figure 8:** Typical SEM-images of the outer surface of samples from the E110opt alloy in the initial state after oxidation in 800/5000 mode.

### High temperature oxidation (800/5000)

The difference in the state of oxide films after oxidation in the 800/5000 mode is established. As can be seen from a comparison of the oxide films surface structure at two magnifications, shown at figures 8 and 9, the film on the initial samples has extended microcracks of width up to  $\sim 3\text{-}4 \mu\text{m}$ , which form a grid, and on polished samples the cracks are practically absent, the width of individual cracks does not exceed  $\sim 0.5\text{-}0.7 \mu\text{m}$ .

The study of the oxide layers transverse structure shows that ion polishing of the samples surface contributes not only to maintaining the integrity of the oxide, but also to reducing the defectiveness of the film in comparison with the initial samples,

increasing its homogeneity, reducing the number of discontinuities and their dimensions, which is clearly seen when comparing figures 10a and 10b. In general, differences in the structure and thickness of oxide films are playing role in oxide protective characteristics. The effect of ion polishing is manifested in a total specific weight gain decrease from  $2.1 \pm 0.1 \text{ mg/cm}^2$  to  $1.7 \pm 0.1 \text{ mg/cm}^2$ , the ECR parameter from  $3.3 \pm 0.1\%$  to  $2.7 \pm 0.1\%$ , the thickness of the oxide layer on the outer surface - from  $12.0 \pm 0.5 \text{ }\mu\text{m}$  to  $9.0 \pm 0.5 \text{ }\mu\text{m}$ .

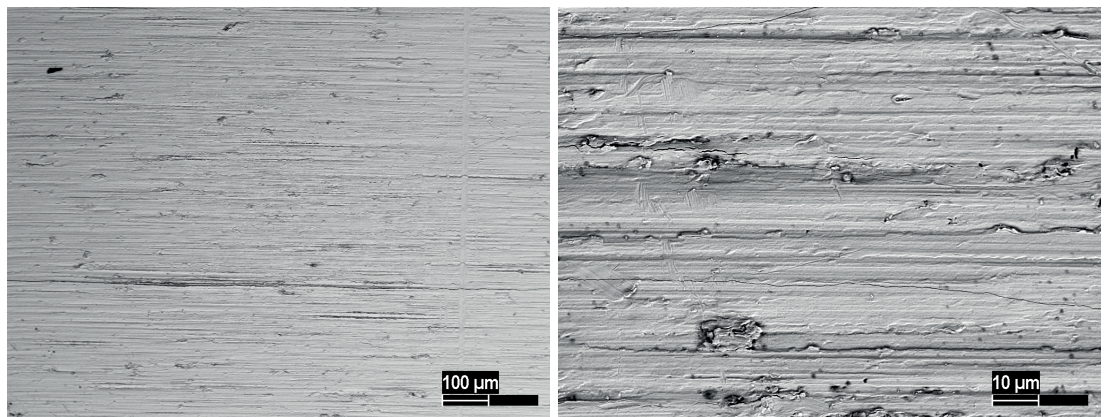


**Figure 9:** Typical SEM-images of the outer surface of samples from the E110opt alloy after ion polishing and oxidation in 800/5000 mode.

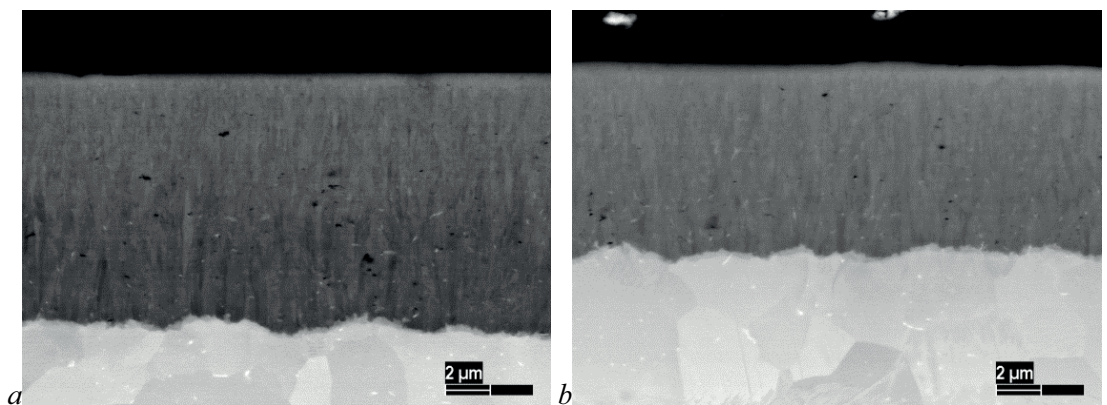


**Figure 10:** Typical SEM-images of the transverse structure of oxide films on E110opt alloy samples in the initial state (a) and after ion polishing (b) after oxidation in 800/5000 mode.

## Alloying in ion mixing mode

The content of alloying elements near the surface of ion-modified samples is about units of atomic percent for iron and up to one atomic percent for other elements and their combinations, as can be seen from the X-ray microanalysis data presented in Table 1. The amount of impurities found in the material, is within the background values.

TABLE 1: Results of X-ray microanalysis of the samples surface after doping by ion mixing of deposited films.

Element content, at.%	initial	Fe doped	Fe+Mo doped	Fe+Y doped
Zr	98,9	96,1	98,2	98,4
Nb	1,1	0,9	0,8	0,8
Fe	-	2,0	0,4	0,4
Mo	-	-	0,6	-
Y	-	-	-	0,4
Pre-deposited film, nm	no	150 (Fe)	70 (Fe+Mo)	90 (Fe+Y)

## Autoclaving

The alloying of the samples from E110opt alloy outer surface by Fe, Fe+Mo, Fe+Y atoms in ion mixing regime slows the oxide layer growth under autoclave conditions, as shown by the analysis of the gravimetric data presented in Figure 11. There are following value of the average specific weight gain decrease compared to initial samples: alloying Fe - by 13%; alloying Fe+Mo - by 39%; alloying Fe+Y - by 35%. The maximum effect is shown by a group of samples doped Fe+Y atoms with additional coating of  $Y_2O_3$  up to 1  $\mu m$  thick. In this case, the reduction in the weight gain was 76%, oxide films have a characteristic dark color without any signs of cracking, flaking and other defects.

## High temperature oxidation (800/5000)

High-temperature corrosion tests of doped samples have shown that the introduction of Fe atoms into the near-surface layer has a positive effect on protective properties of the forming oxide film, reducing its defectiveness and corrosion rate. This can be seen from a comparison of the images of the transverse metallographic sections in Figure 12. As a consequence, the total specific weight gain of samples doped with Fe in comparison with the samples in the initial state decreases from  $2.1 \pm 0.1 \text{ mg/cm}^2$  to  $1.9 \pm 0.1 \text{ mg/cm}^2$ , the ECR parameter - from  $3.3 \pm 0.1\%$  to  $3.0 \pm 0.1\%$ , the thickness of the oxide layer on the outer surface - from  $12.0 \pm 0.5 \mu m$  to  $10.0 \pm 0.5 \mu m$ .

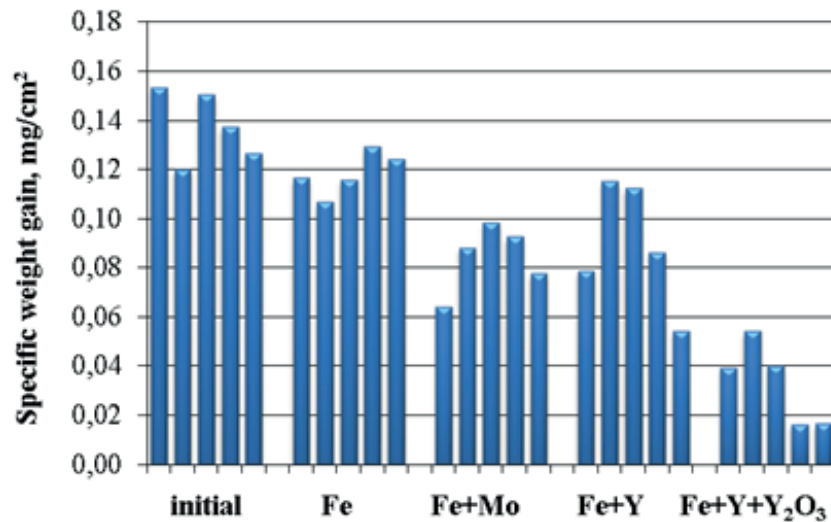


**Figure 11:** Specific weight gain of samples in the initial state doped with Fe, Fe+Mo, Fe+Y and Fe+Y doped with  $Y_2O_3$  coating obtained after autoclaving for 400 hours.

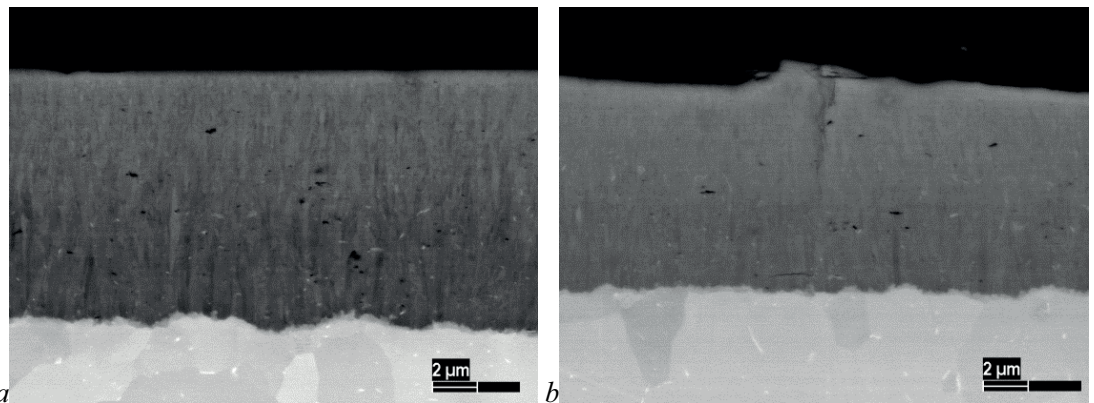


**Figure 12:** Typical SEM-images of the transverse structure of oxide films on samples of the alloy E1100p in the initial state (a) and doped Fe (b) after oxidation in 800/5000 mode.

## Coated samples

Corrosion tests were carried out on samples with coatings of Cr and FeCrNi in 800/5000, 800/7500, 1000/5000 modes.

## High temperature oxidation (800/5000)

Analysis of the results showed that the most effective from the viewpoint of corrosion resistance of the alloy increasing is coating from FeCrNi atoms 2-4  $\mu\text{m}$  thick. As can be seen from Figure 13, after oxidation in the 800/5000 mode, there are no large cracks on the oxide surface, the width of small cracks does not exceed  $\sim 0.3\text{-}0.5 \mu\text{m}$ , and the length is  $\sim 10\text{-}30 \mu\text{m}$ . Analysis of the oxygen distribution over the thickness of

the samples showed that the coating of FeCrNi completely blocks the penetration of oxygen into the metal. However, the presence of cracks in the oxide, as seen in Figure 14, leads to the formation of local areas of zirconium oxide, with the possible translation of the crack into the metal. The total specific weight gain of FeCrNi-coated samples 2-4  $\mu\text{m}$  thick as compared to the samples in the initial state decreases from  $2.1 \pm 0.1 \text{ mg/cm}^2$  to  $1.7 \pm 0.1 \text{ mg/cm}^2$ , the ECR parameter from  $3.3 \pm 0.1\%$  to  $2.7 \pm 0.1\%$ .

### High temperature oxidation (800/7500)

Increase of the corrosion tests duration at 800 °C up to 7500 s results in the cracks in oxide on the initial samples expanding and forming a closed grid, which is likely to lead to peeling of film and strong acceleration of corrosion. Visually, surface of samples coated with FeCrNi atoms 2-4  $\mu\text{m}$  thick remains homogeneous, as can be seen from the comparison of figures 15a and 15b. Under these conditions, total specific weight gain of the coated samples as compared to the initial samples decreases from  $3.3 \pm 0.1 \text{ mg/cm}^2$  to  $2.5 \pm 0.1 \text{ mg/cm}^2$ , ECR decreases from  $5.1 \pm 0.1\%$  to  $3.9 \pm 0.1\%$ .

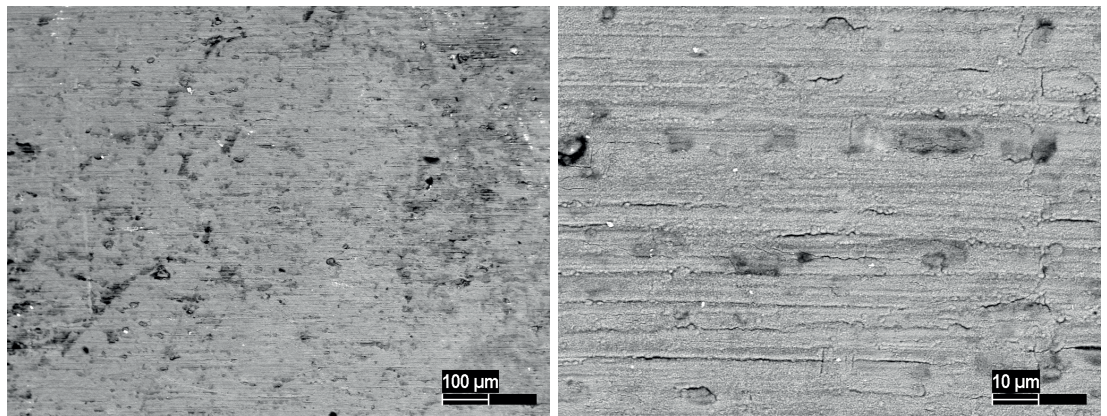


**Figure 13:** Typical SEM-images of the outer surface of samples from the E110opt alloy coated with FeCrNi atoms 2-4  $\mu\text{m}$  thick after oxidation in 800/5000 mode.

### High temperature oxidation (1000/5000)

As a result of oxidation in 1000/5000 mode of initial samples and samples coated with FeCrNi atoms 2-4  $\mu\text{m}$  thick, as seen in Figure 16, an oxide film is formed without visible traces of destruction. The total specific weight gain of coated samples as compared with the samples in the initial state decreases from  $5.3 \pm 0.1 \text{ mg/cm}^2$  to  $5.1 \pm 0.1 \text{ mg/cm}^2$ , ECR decreases from  $8.4 \pm 0.1\%$  to  $8.1 \pm 0.1\%$ .

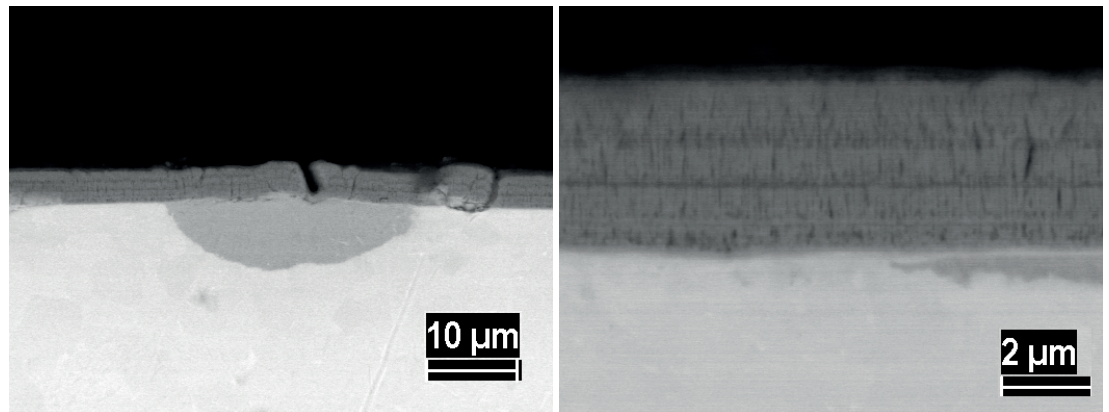


**Figure 14:** Typical SEM-images of the transverse structure of oxide films on samples of the E110opt alloy coated with FeCrNi atoms 2-4  $\mu\text{m}$  thick after oxidation in 800/5000 mode.

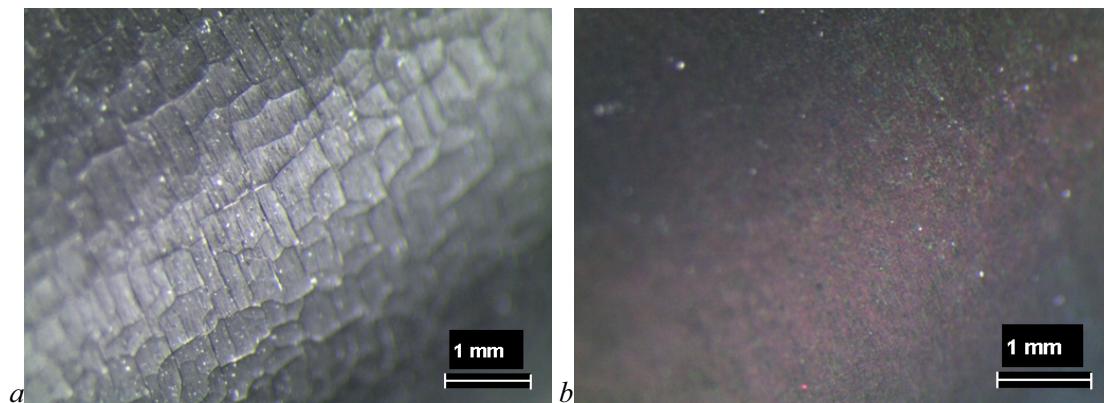


**Figure 15:** Typical images of the outer surface of samples of the E110opt alloy in the initial state (a) and with a coating of FeCrNi atoms 2-4  $\mu\text{m}$  thick (b) after oxidation in 800/7500 mode.

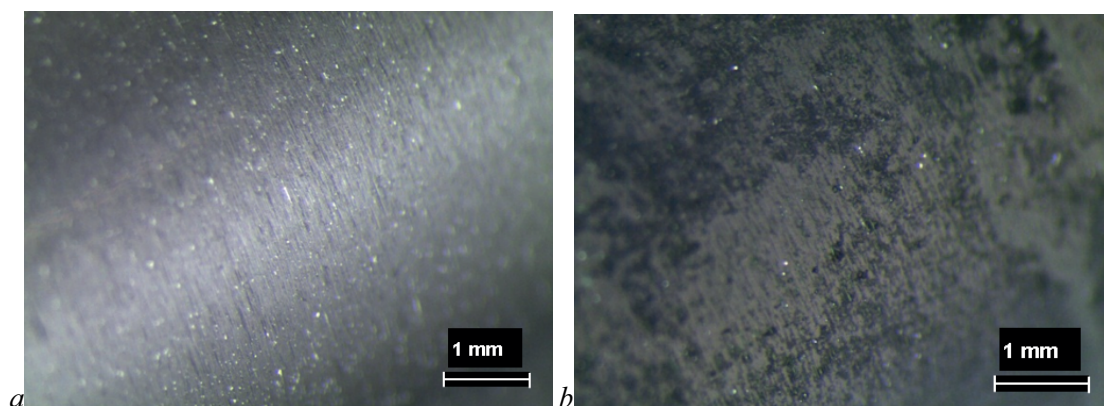


**Figure 16:** Typical images of the outer surface of samples from the alloy E110opt in the initial state (a) and with a coating of FeCrNi atoms 2-4  $\mu\text{m}$  thick (b) after oxidation in 1000/5000 mode.

## 4. DISCUSSION

Modification of the E110opt alloy near-surface layer gives positive results of decreasing weight gain in autoclaving and high temperature oxidation at 800 °C. Positive effect of

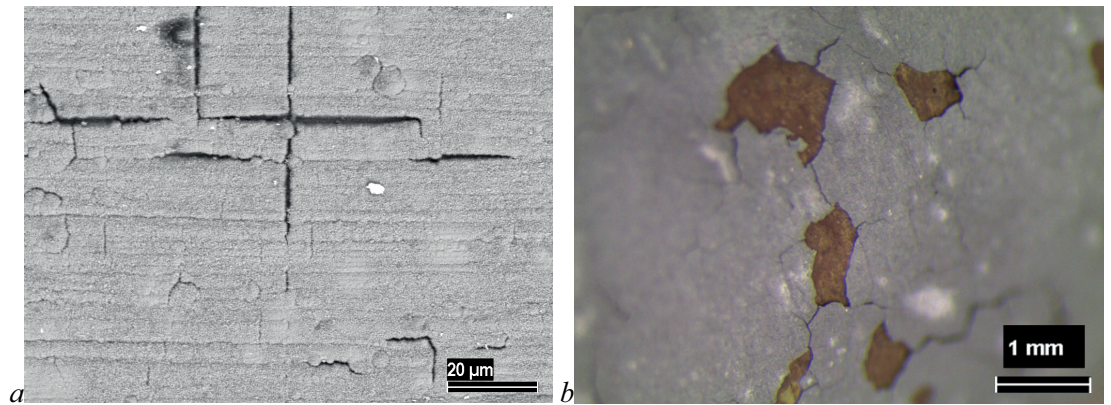


**Figure 17:** Typical images of the outer surface of samples with Cr coatings 2-4  $\mu\text{m}$  thick (*a* - 800/5000 oxidation, SEM image) and 8  $\mu\text{m}$  (*b* - oxidation 1000/5000, optical image).

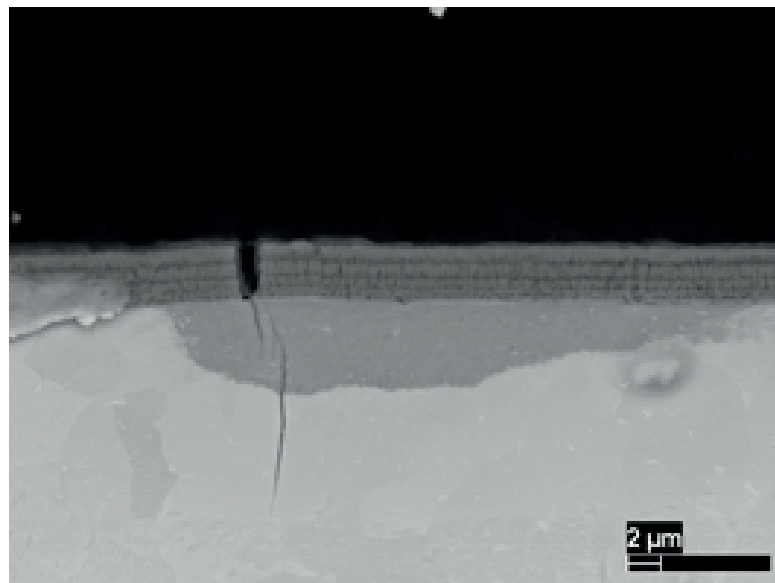


**Figure 18:** SEM image of the E110opt sample outer surface coated by FeCrNi atoms 2-4  $\mu\text{m}$  thick after oxidation in 800/5000 mode near the crack.

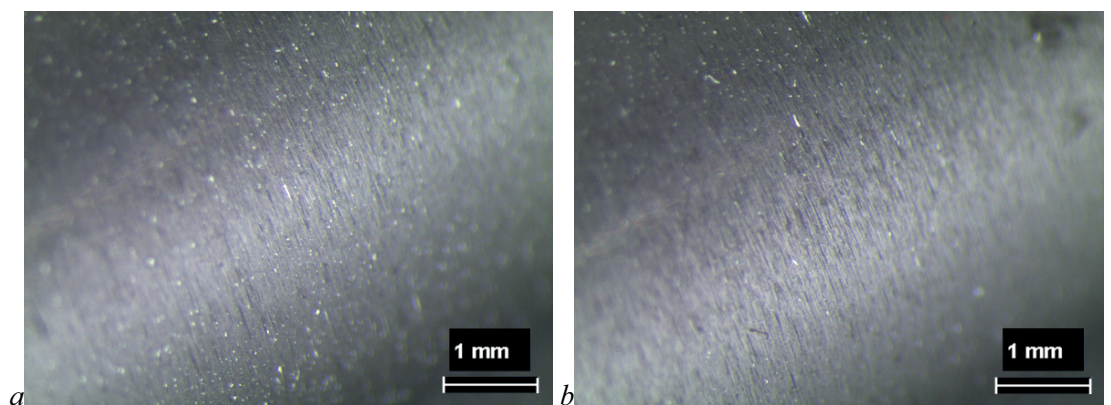


**Figure 19:** Typical images of the transverse structure of oxide films on samples of the alloy E110opt in the initial state (*a*) and doped Fe (6) after oxidation in 1000/5000 mode.

ion polishing on the defectiveness of oxide films is due to decrease surface roughness, smoothing of the defects of the tubes rolling process and accompanied by decrease in density of growth defects in the oxide as pores and microcracks and their size. The beneficial effect of ion polishing on the growth of oxide films has been shown previously [5, 6].

Autoclaving of the samples under conditions close to the operational ones for WWER (water temperature 350 °C, pressure 16.5 MPa with exposure to 400 h) made it possible to note a significant decrease of average specific weight gain on the modified samples in comparison with initial samples: ion polishing - by 49%; alloying Fe - by 13%; alloying Fe+Mo - by 39%; alloying Fe+Y - by 35%; alloying Fe+Y + coating  $Y_2O_3$  - by 76%. In addition, there are practically no cracks that are observed on samples with an untreated surface on the surface of samples that have undergone ion polishing and iron doping, after the high-temperature oxidation in 800/5000. This confirms the previously established results about possibility of significant increase of zirconium alloys corrosion resistance at operational conditions by ion-beam modification methods.

Alloys with FeCrNi coating have the best resistance to the destruction of oxide films at temperature 800 °C. The Cr coatings that we have created are not effective barrier for the penetration of oxygen into the metal. There are stratification of chromium coatings, in the studied thicknesses from 2-4  $\mu\text{m}$  to 8  $\mu\text{m}$  at 800 °C, which at 1000 °C results with the detachment of chromium oxide fragments, as is clearly seen in Figure 17*a* and *b*, respectively.

Negative effects of cracks formed in the coatings should be noted. As can be seen in Figure 18, oxygen penetrates to the zirconium along the crack in the coating during oxidation, and near the crack an intense zirconium oxidation zone is formed. Crack passes from the coating oxide to the zirconium oxide and further into the metal, creating a threat of cladding destruction.

According to the high-temperature oxidation conditions, samples heating to temperatures of 1000 °C and 1200 °C passed fairly quickly and E110opt alloy was in the  $\beta$ -phase state during oxidation. Cracks in the oxides were absent on all samples, apparently, firstly, due to the intensive diffusion processes of components redistribution and healing of cracks formed during heating and, secondly, due to the possible relaxation of thermal stresses by plastic deformation in oxide. Therefore, oxide films on the initial (figure 19*a*) and modified samples (Figure 19*b*) during oxidation at 1000 °C for 5000 s, visually have a dense structure and specific dark color of  $ZrO_2$ . It is important to emphasize that oxide film on the sample with FeCrNi coating surface also retains its

integrity and has a dark color., Continuous oxide film is formed on both initial, ion-polished and iron-doped samples during oxidation at 1200 °C for 1000 s, and samples with an ion-polished surface should be visually preferred.

From the different modified samples, samples that were subjected to ion polishing, alloying with iron atoms, and also with FeCrNi coating turned out to be better than the initial state at high temperature oxidation with temperatures of 800, 1000 and 1200 °C.

## 5. CONCLUSION

It is shown, that smoothing of the surface relief as a result of ion polishing by a radial beam  $Ar^+$  up to  $Ra < 0.3 \mu m$  helps to reduce the defectiveness of the oxide film during oxidation in autoclave conditions (water, 350 °C, 16.5 MPa, 400 h). That positively affects its protective properties - the oxide thickness decreases from  $12.0 \pm 0.5 \mu m$  to  $9.0 \pm 0.5 \mu m$ . Considering the negative impact of fuel rods surface technological defects on the formation of a protective oxide film, serious attention should be given to the possibilities of claddings or fuel rods ion polishing sold on industrial scale.

It is established that material surface doping in ion mixing mode by Fe, Fe+Mo, Fe+Y atoms increases the corrosion resistance of the E110opt alloy in autoclave conditions (water, 350 °C, 16.5 MPa, 400 h) - the oxide layer thickness decreased by 13%, 39% and 35%, respectively. The maximum effect of slowing down the corrosion rate was observed when the surface was doped with Fe+Y atoms with additional deposition of the  $Y_2O_3$  film - the thickness of oxide layer decreases average by 76% compared to the samples in initial state.

It was found that ion polishing and doping of the surface of samples by Fe atoms suppresses the cracking of the oxide upon vapor oxidation at 800 °C up to 5000 s and helps to reduce the film defectiveness, namely, the number of micropores and discontinuities in the body of the oxide and their dimensions. This increases film protective properties and leads to decrease of ECR from  $3.3 \pm 0.1\%$  to  $2.7 \pm 0.1\%$  and  $3.0 \pm 0.1\%$ , respectively.

It is shown that magnetron deposited coating of FeCrNi of 2-4  $\mu m$  a thickness effectively inhibits oxygen penetration into the metal from vapor environment under close to LOCA conditions, increasing the corrosion resistance of the alloy E110opt. The coating maintains its integrity during oxidation at 800 °C with exposure up to 5000 s and 7500 s, and at 1000 °C with exposure up to 5000 s. While there is active cracking of the oxide on initial samples, which obviously has a negative effect on its protective properties, only a small number of cracks have been found on FeCrNi coated samples, near which local

regions of zirconia are formed (ECR decreases from  $3.3 \pm 0.1\%$  to  $2.7 \pm 0.1\%$  at 800/5000, from  $5.1 \pm 0.1\%$  to  $3.9 \pm 0.1\%$  at 800/7500 and from  $8.4 \pm 0.1\%$  to  $8.1 \pm 0.1\%$  at 1000/5000 oxidation mode).

## ACKNOWLEDGMENTS

This work was supported by the MEPhI Academic Excellence Project (agreement with the Ministry of Education and Science of the Russian Federation of August 27, 2013, project no. 02.a03.21.0005).

## References

- [1] Valikov R.A., Yakutkina T.V., Kalin B.A., Volkov N.V., Krivobokov V.P., Yanin S.N., Asainov O.Kh., Yur'yev Yu.N., Yashin A.S. // Journal of Physics: Conference Series 652 (2015), 012068
- [2] Kalin B.A., Volkov N.V., Valikov R.A., Yashin A.S. // Bulletin of the Russian Academy of Sciences: Physics. 2014, 78 (6), pp. 553-557.
- [3] S.S. Bazyuk, I.A. Deryabin, D.S. Kiselev, Yu.A. Kuzma-Kichta, A.A. Mokrushin, N.Ya. Parshin, Ye.B. Popov, D.M. Soldatkin // Proceedings of Conference MNTK-2017, Podolk, Russia, 2017.
- [4] Waterside corrosion of zirconium alloys in nuclear power plants. IAEA-TECDOC-996, Vienna, Austria, 1998.
- [5] B. A. Kalin, N. V. Volkov, R. A. Valikov, A. S. Yashin // Inorganic Materials: Applied Research, 2017, Vol. 8, No. 3, pp. 364-369.
- [6] Kalin B.A., Volkov N.V., Valikov R.A., Yashin A.S. // IOP Conf. Series: Materials Science and Engineering 130 (2016) 012005